# PLA/PBAT blends for blown film extrusion

**Justyna Ostrowska**[1), *)] (ORCID ID: 0000-0003-1777-7214), **Waldemar Sadurski**[1)] (0000-0002-5919-3754), **Magdalena Paluch**[1)] (0000-0003-1491-9723), **Maciej Dębowski**[2)] (0000-0001-5405-8433), **Olga Wrona**[1)] (0000-0003-1135-6849), **Karolina Sołtan**[1)] (0000-0002-2098-9579), **Piotr Tyński**[1)] (0000-0003-1647-7455)

DOI: https://doi.org/10.14314/polimery.2024.7.4

**Abstract**: Films of biodegradable PLA/PBAT blends with PBAT content of 10–90 wt% were obtained by extrusion blowing. PLA/PBAT blends were characterized by FT-IR, DSC, TGA and SEM. Tensile properties and tear strength of the films were also determined. It was shown that despite thermodynamic immiscibility of PLA and PBAT, addition of PBAT in amounts above 50 wt% allows obtaining films with good functional properties. Optimal properties were obtained with PBAT content of 60 or 70 wt%. Tensile strength was 36.7–38.7 MPa, elongation at break 357–388% and tear strength 11–22 N/mm.

**Keywords**: PLA/PBAT blends, blown film extrusion, thermal properties, morphology, mechanical properties.

## Mieszaniny PLA/PBAT do wytłaczania folii z rozdmuchiwaniem

**Streszczenie**: Metodą wytłaczania z rozdmuchiwaniem otrzymano folie z biodegradowalnych mieszanin PLA/PBAT, w których zawartość PBAT wynosiła 10–90% mas. Mieszaniny PLA/PBAT scharakteryzowano za pomocą FT-IR, DSC, TGA i SEM. Określono również właściwości mechaniczne przy rozciąganiu i wytrzymałość na rozdzieranie folii. Wykazano, że pomimo termodynamicznej niemieszalności PLA i PBAT, dodatek PBAT w ilości powyżej 50% mas. umożliwia otrzymanie folii o dobrych właściwościach użytkowych. Optymalne właściwości uzyskano przy zawartości PBAT wynoszącej 60 lub 70% mas. Wytrzymałość na rozciąganie wynosiła 36,7–38,7 MPa, wydłużenie przy zerwaniu 357–388%, a wytrzymałość na rozdzieranie 11–22 N/mm.

**Słowa kluczowe:** mieszaniny PLA/PBAT, wytłaczanie folii z rozdmuchiwaniem, właściwości termiczne, struktura, właściwości mechaniczne.

Polylactide (PLA) is one of the most popular commercially available biodegradable polyesters. In terms of properties, PLA is compared to polystyrene or poly(etylene terephtalate) (PET) hence, it is the object of packaging industry [1]. Standard-grade PLA has high Young's modulus (3 GPa) and tensile strength in the range 50–70 MPa, but extremely low elongation at break (≤ 3%) [2]. The PLA application has been limited due to its low fracture toughness and flexibility, high brittleness, slow crystallization, low glass transition temperature and thermal stability, as well narrow processing window. Consequently, the use of PLA in blown film extrusion, which is the most important industrial process in the production of polymeric films for packaging is restricted [3, 4]. The mentioned limitation of polylactide could be overcome by addition of viscosity enhancers and compatibilizers, such as plasticizers and reactive coupling agents or copolymerization [5–9]. However, the most popular and easiest methods to achieve improvements in PLA properties is blending with other flexible biodegradable polymers, such as poly(butylene succinate) (PBS), poly(butylene succinate-*co*-adipate) (PBSA) and poly(butylene adipate-*co*-terephtalate) (PBAT) [10]. The last one copolyester has been considered as a good alternative to toughening PLA. The mechanical properties of PBAT are like low density polyethylene which make it suitable for blowing film application. The tensile strength of PBAT is 21 MPa and the elongation at break is 670%, as well the flexural modulus is 126 MPa. On the other hand, applications of neat PBAT have been limited by high cost or low stiffness. Thus, a blending of PLA and PBAT is a good solution to obtain biodegradable materials with complementary properties derived from pristine polymers and obtain blends with optimal properties which can be processed by blown extrusion to produce thin films for packaging industry [11].

The literature is very scarce and incomplete with respect to PLA/PBAT blends blown films. Previous research indicates that the optimal composition for processing to obtain flexible films is a PLA/PBAT (80 wt%/20 wt%) [12–14].

---

[1)] Łukasiewicz Research Network – New Chemical Syntheses Institute, Biodegradable Plastics Research Group, Aleja Tysiaclecia Panstwa Polskiego 13a, 24-110 Pulawy, Poland.

[2)] Warsaw University of Technology, Faculty of Chemistry, Noakowskiego 3, 00-664 Warsaw, Poland.

[*)] Author for correspondence:
justyna.ostrowska@ins.lukasiewicz.gov.pl

Hongdilokkul *et al.* [12] prepared the films by blown extrusion method from PLA/PBAT blends at the weight ratio of 80:20 together with and without peroxide as reactive agent. The results showed that mechanical properties of PLA/PBAT blends insignificantly improved after being modified by peroxide with concentration 0.02 and 0.0002 phr. According to Jiang *et al.* [14] the 20 wt% PBAT content in the blend led to significantly increase the elongation at break of PLA, namely from 4% to 200%. However, there is no complete characterization as to the necessary content of PBAT to obtain films in a continuous and stable technological extrusion blown film process. Su *et al.* [15] obtained and analyzed a series of PLA/PBAT granulates with PBAT content from 10% to 90%, then further processed to obtain films. However, extrusion blown films were successfully obtained only for blends in which the PBAT content is at least 60 wt%.

The PLA/PBAT are thermodynamically immiscible [14]. Although morphological and DMA analysis of PLA/PBAT specimens reveal that PBAT molecules are miscible with PLA molecules at PBAT contents equal to or less than 2.5 wt% as no phase separation occurs [16]. It is possible to improve the compatibility of PLA/PBAT blends intended to obtain films with better mechanical properties by reactive extrusion with appropriate additives. Su [17] used tetrabutyl titanate as a catalyst to prepare masterbatch for the compatibilized PLA/PBAT compatibilization of the (20/80 wt%) blend. Another well-known solution is incorporation into the blends a multifunctional epoxy chain extender, such as commercial Joncryl® [18, 19].

Therefore, in this work, the possibility of obtaining blown films from PLA/PBAT blends, in which PBAT content varies by 10 wt% in the range of 10–90 wt%, was investigated. PLA/PBAT blends obtained by twin-screw extrusion were subjected to spectroscopic and thermal analysis using FT-IR, DSC and TGA methods to assess their compatibility and thermal stability. Moreover, the obtained films were subjected to tensile and tear strength tests and their morphology was assessed using SEM.

## EXPERIMENTAL PART

### Materials

PLA (IngeoTM Biopolymer 2003D) with a melt flow rate of MFR = 6 g/10 min (210°C, 2.16 kg) and a specific gravity of 1.24 g/cm$^3$ was supplied by NatureWorks LLC (Minnetonka, USA). PBAT (Ecoflex F Blend C1200) with a melt flow rate of MFR = 2.7–4.9 g/10 min (190°C, 2.16 kg) and a bulk density of 1.25–1.27 g/cm$^3$ was purchased from BASF SE (Ludwigshafen, Germany).

### PLA/PBAT blends preparation

PLA and PBAT were dried prior to extrusion for 4 h at 85°C and 65°C, respectively. PLA/PBAT blends containing 10, 20, 30, 40, 50, 60, 70, 80 or 90 wt% PBAT were obtained by melt mixing using a twin-screw extruder (Labtech Engineering Company Ltd, Thailand) with a screw diameter of 26 mm and an *L*/*D* ratio of 52. The process was carried out under the following conditions: screw speed of 120 rpm, flow rate of 8 kg/h and barrel temperature from the feed zone to the die zone in the range of 170–190°C. Pure PLA and PBAT were extruded under the same conditions to compare their thermal properties before and after extrusion. The processed PLA and PBAT were named PLA(p) and PBAT(p), respectively. The extrudates were cooled in an air stream and cut into pellets using a side-cut pelletizer. The obtained PLA/PBAT blends were stored in airtight containers at room temperature.

### PLA/PBAT films manufacturing

PLA/PBAT blends were processed using laboratory blown film line (LF-250 Labtech Engineering Company Ltd, Thailand) in combination with a single screw extruder (LE20-30, $D = 20$ mm and $L/D = 30$, Labtech Engineering Company Ltd, Thailand) to obtain films. The extrusion temperature of the blown film of PLA/PBAT blends from the hopper to the die was in the range of 170–200°C depending on the composition of the blend. The screw speed, which determined the extrusion throughput, was 90 rpm. The speed of the nip roll and the winding speed were 2.3 m/min. The extrusion melt pressure was in the range of 240–340 bar. The main processing parameters used to illustrate melt orientation during film blowing are the blow-up ratio (*BUR*) and the draw down ratio (*DDR*) [15, 20]. BUR indicates the increase in the bubble diameter ($D_b$) over the die diameter ($D_d$), defined as:

$$\mathrm{BUR} = D_b/D_d \tag{1}$$

where $D_d$ is 37 mm and $D_b$ was calculated by Equation (2) from the lay flat width as follows:

$$D_b = 2 \times \text{Lay flat width} / \pi \tag{2}$$

The final thickness reduction in the melt after blowing is indicated by a draw down ratio (*DDR*) according to Equation (3):

$$DDR = \text{Die gap} / (\text{Film thickness} \times \mathrm{BUR}) \tag{3}$$

where the die gap was 0.8 mm.

### Methods

#### Fourier transform infrared spectroscopy (FT-IR)

Infrared spectra were recorded on a Nicolet iS10 FT-IR spectrometer manufactured by Thermo Scientific (Waltham, USA) using the Attenuated Total Reflection (ATR) technique with a laminated diamond crystal at room temperature with a resolution of 4 cm$^{-1}$ in the spectral range of 650–4000 cm$^{-1}$.

### Differential scanning calorimetry (DSC)

DSC measurements were performed in a nitrogen atmosphere using a TA Instruments Q20 (New Castle, USA) equipped with a cooling system (RCS90, TA Instruments, New Castle, USA). The sample (10 mg) was placed in an aluminum pan with a hermetic seal and then in the measuring cell. Three thermal cycles were used. The samples were first cooled to -90°C at a rate of 5°C/min, then heated to 180°C at a rate of 5°C/min and held at this temperature for 1 min. Then, they were cooled to -90°C at a rate of 5°C/min and reheated to 180°C at a rate of 5°C/min. The glass transition temperature ($T_g$), cold crystallization temperature ($T_{cc}$), melting temperature ($T_m$) and degree of crystallinity of PLA ($c_c$) calculated according to equation (4) were determined from the second heating scan.

$$c_c = [\Delta H_m/(w_{PLA} \times \Delta H_{m,100\%})] \times 100\% \quad (4)$$

where: $\Delta H_m$, J/g – the measured enthalpy of melting of PLA, $w_{PLA}$ – weight fraction of PLA in the blends, $\Delta H_{m,100\%}$ = 93.7 J/g – the heat of fusion of 100% crystalline PLA [21].

### Thermogravimetric analysis (TGA)

TGA analysis was performed on a TA Instruments Q50 thermogravimeter (New Castle, USA) under nitrogen atmosphere. The sample (10 mg) was placed in a platinum pan, put into a TGA furnace, and heated at the constant rate of 10°C/min in the temperature range of 25–480°C. The change in weight as a function of temperature was recorded. Start ($T_{onset}$) and end ($T_{endset}$) temperatures of decomposition were determined. Additionally, based on the differential thermogravimetric curve, which is the first derivative of the TG curve, the maximum decomposition rate temperature ($T_{max}$) was determined. The maxima visible on DTG curve correspond to $T_{max}$.

### Scanning electron microscopy (SEM)

SEM images were taken using a Helios 5 PFIB scanning electron microscope (Thermo Fisher Scientific, Hillsboro, OR, USA) equipped with a high-resolution Elstar field emission column, a Phoenix ion column with inductively coupled Xe+ plasma, and a set of Elstar detectors for secondary electrons (standard ETD detector placed in the chamber) and intracolumn TLDs (for high-resolution immersion imaging), an ABS/CBS scattered electron detector, a STEM3+ detector, and an ICE detector for ion imaging. A working distance of about 4.0 mm and an electron beam acceleration voltage of 5 kV were used. Before measurement, all samples were fractured at liquid nitrogen temperature, and after warming to room temperature, a 10 nm thick Au layer was sputtered using a CCU-010 high-vacuum sputtering unit (Safematic GmbH, Zizers, Switzerland).

### Mechanical properties

Static tensile properties were measured in accordance with PN-EN ISO 527 on an Instron 3345 series single-column testing machine with Bluehill 3 software (Norwood, USA). Test strips approximately 200 mm long and 15 mm wide were cut from a representative part of

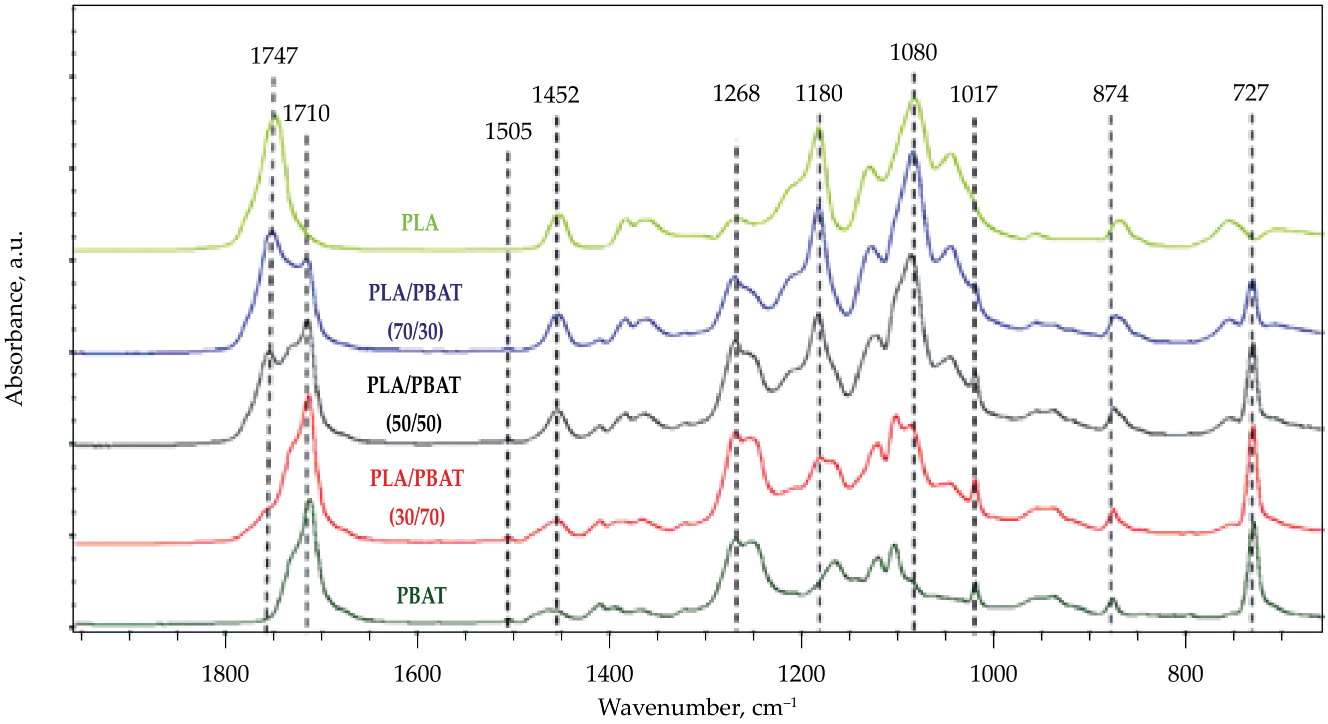

**Fig. 1. FT-IR spectra of PLA, PBAT and PLA/PBAT blends**

**T a b l e 1. DSC data of PLA, PBAT and their blends**

| PLA/PBAT wt%/wt% | PLA phase | | | | | | PBAT phase | |
|---|---|---|---|---|---|---|---|---|
| | $T_g$, °C | $T_{cc}$, °C | $T_{m1}$, °C | $T_{m2}$, °C | $\Delta H_m$, J/g | $c_c$, % | $T_g$, °C | $T_m$, °C |
| PLA | 59.3 | 118.2 | – | 154.3 | 7.9 | 8.4 | – | – |
| PLA(p) | 57.3 | 103.9 | 147.2 | 154.8 | 27.8 | 29.7 | – | – |
| 90/10 | 56.5 | 105.3 | 146.0 | 152.2 | 24.8 | 29.4 | –36,2 | – |
| 80/20 | 57.0 | 105.1 | 146.1 | 152.2 | 22.8 | 30.4 | –34.7 | – |
| 70/30 | 58.1 | 109.0 | 147.0 | 151.2 | 18.0 | 27.4 | –34.0 | – |
| 60/40 | 57.8 | 112.1 | 147.4 | – | 15.3 | 27.2 | –32.9 | – |
| 50/50 | 58.0 | 115.9 | 148.2 | – | 12.1 | 25.8 | –32.2 | – |
| 40/60 | 58.2 | 116.1 | 148.3 | – | 9.8 | 26.1 | –33.3 | – |
| 30/70 | 58.5 | 115.4 | 148.3 | – | 6.4 | 22.8 | –32.1 | 128.2 |
| 20/80 | 58.4 | 113.1 | 148.3 | – | 3.4 | 18.1 | –31.8 | 128.5 |
| 10/90 | 57.9 | – | 147.5 | – | – | – | –32.2 | 121.2 |
| PBAT(p) | – | – | – | – | – | – | –32.8 | 125.0 |
| PBAT | – | – | – | – | – | – | –30.3 | 121.6 |

the film along extrusion direction. The crosshead speed was of 100 mm/min. The tear strength of the film was determined by the Elmendorf method using an electronic ProTear® tester (Thwing-Albert Instruments Company, West Berlin, USA). Measurements were performed in accordance with PN-EN ISO 6383-2 for samples with a constant radius (43±0.5 mm) in the direction of film extrusion and a length of 75±0.5 mm. Pendulums weighing 200 g and 1600 g were used for the measurements. All samples subjected to mechanical tests were conditioned in a climatic chamber at a temperature of 23°C and humidity of 50% for 24 h before the measurements.

## RESULTS AND DISCUSSION

### FT-IR analysis

FT-IR spectroscopy was performed to analyze chemical structure of PLA, PBAT and PLA/PBAT blends. Fig. 1 presents PLA and PBAT spectra with characteristic absorption bands. Intensity of carbonyl group bands located around 1710 cm$^{-1}$ for PBAT and 1747 cm$^{-1}$ for PLA, changed without their shift depending on the respective polyester content in the blend. Thus, there are no strong interactions between biodegradable polyesters, regardless of the composition of the blend, which are considered immiscible [22]. Additionally, bands characteristic for phenylene groups could also be observed, e.g., stretching C=C bands located in the 1500–1450 cm$^{-1}$ region, as well as signals at 727 cm$^{-1}$ and 874 cm$^{-1}$ ascribed to the out of plane bending modes. The other characteristic absorption bands of polylactide in PLA/PBAT blends also included those with the maxima at 1452 cm$^{-1}$ (C-H deformation in $CH_3$), 1268–1140 cm$^{-1}$ (C-O stretching in C-O-C group, partially overlapping with PBAT bands).

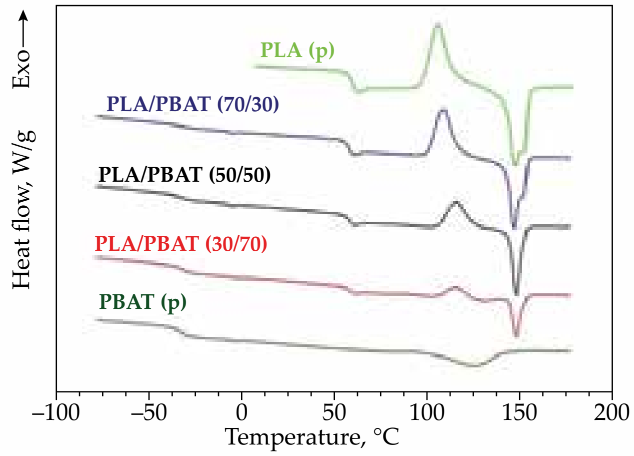

**Fig. 2. DSC second heating run curves of PLA/PBAT blends**

### Thermal properties

Table 1 and Fig. 2 presents DSC results for PLA/PBAT blends compared to neat and processed polyesters. Pure PLA before and after processing had a higher melting point than in the blends. In the case of PLA/PBAT blends, the melting region of PBAT overlapped with the cold crystallization region of PLA. Therefore, it was not possible to determine the melting temperature of PBAT in blends with PLA content higher than 30 wt%. Blends containing 10–30 wt% PBAT showed double PLA melting peaks, which could be attributed to lamellar reorganization [6]. All blends showed two separate glass transition temperatures related to the PLA and PBAT phase in the blends without significant change compared to pure PLA and PBAT, indicating the polymers thermodynamic immiscibility. Xiao also presented this conclusion *et al.* [23] who studied PLA/PBAT blends (80/20, 60/40 and 40/60). The

**Table 2. TGA data for PLA, PBAT and their blends**

| PLA/PBAT wt%/wt% | PLA | | | PBAT | | |
|---|---|---|---|---|---|---|
| | $T_{onset}$ °C | $T_{endset}$ °C | $T_{max}$ °C | $T_{onset}$ °C | $T_{endset}$ °C | $T_{max}$ °C |
| PLA | 350 | 383 | 373 | - | - | - |
| PLA(p) | 344 | 377 | 366 | - | - | - |
| 90/10 | 342 | 378 | 363 | - | - | - |
| 80/20 | 341 | 381 | 363 | - | - | - |
| 70/30 | 341 | 369 | 361 | 392 | 413 | 391 |
| 60/40 | 339 | 364 | 357 | 389 | 414 | 395 |
| 50/50 | 342 | 365 | 360 | 388 | 413 | 395 |
| 40/60 | 339 | 360 | 357 | 386 | 416 | 398 |
| 30/70 | 331 | 363 | 356 | 386 | 416 | 399 |
| 20/80 | 333 | 352 | 358 | 385 | 415 | 399 |
| 10/90 | 323 | 360 | 344 | 380 | 416 | 399 |
| PBAT(p) | - | - | - | 376 | 418 | 402 |
| PBAT | - | - | - | 385 | 424 | 414 |

introduction of PBAT resulted in an increase in $T_{cc}$ and a decrease in the degree of crystallinity of PLA domains, which indicates a poorer ability of PLA to crystallize in blends compared to PLA(p).

The thermal decomposition of PLA, PBAT and PLA/PBAT blends is summarized in Table 2 and shown in Figure 3. TGA of PLA/PBAT blends did not show any significant changes in their thermal stability. TG and DTG curves showed two mass loss transformations for the individual blend phases, which depended on the content of the individual components. The first (low temperature) process is related to PLA degradation, and the second transformation can be attributed to the mass loss associated with PBAT degradation (Fig. 3). However, the temperature regions where these transformations occurred partially overlapped, making it impossible to separate the final PLA degradation temperature from the onset of PBAT thermolysis, especially for the blends with the highest PLA content (> 70 wt%).

In the case of PLA/PBAT blends, PLA was characterized by a lower degradation temperature, so its thermal properties determined the blends thermal stability. As a result of the processing, the $T_{onset}$ temperature of PLA in blends was reduced. $T_{onset}$ of PLA in PLA/PBAT blends was in the range of 323–342°C and was lower compared to PLA. It is worth noting that its value showed some dependence on the composition of the blend. In the case of blends containing ≤ 40 wt% PLA, $T_{onset}$ was only slightly lower (≤ 5°C) than $T_{onset}$ PLA(p). However, in the case of a higher PBAT content, the onset temperature of the blends was significantly lower.

## Analysis of PLA/PBAT blown film processing conditions

It is known that a BUR value greater than 1 indicates that the bubble has been blown to a larger diameter than the die diameter and the film has been thinned and has a transverse direction (TD) orientation. In addition, a DDR greater than 1 indicates that the melt has been pulled away from the die faster than it was extruded and therefore the film has been thinned and has a machine direction (MD) orientation. The blown film extrusion parameters are shown in Table 3.

The blow-up ratio was about 3.7 for all blends containing up to 50 wt% PLA and decreased to about 3.3 for blends with higher PLA content. It is worth noting that the pure PBAT film was sticky after passing the pinch roller, but it was possible to separate flat layers. At PLA contents of 10–40 wt%, the film blowing process was stable and smooth films were obtained. When the PLA content increased to 50 wt%, the resulting film wrinkled slightly after passing the pinch roller, and this phenomenon was intensified with further increase in PLA content. At the same time, the melt strength of the blends decreased, the film bubbles were stable due to higher die temperature and reduced bubble cooling. The processing of the pure PLA blown film was difficult due to the low melt

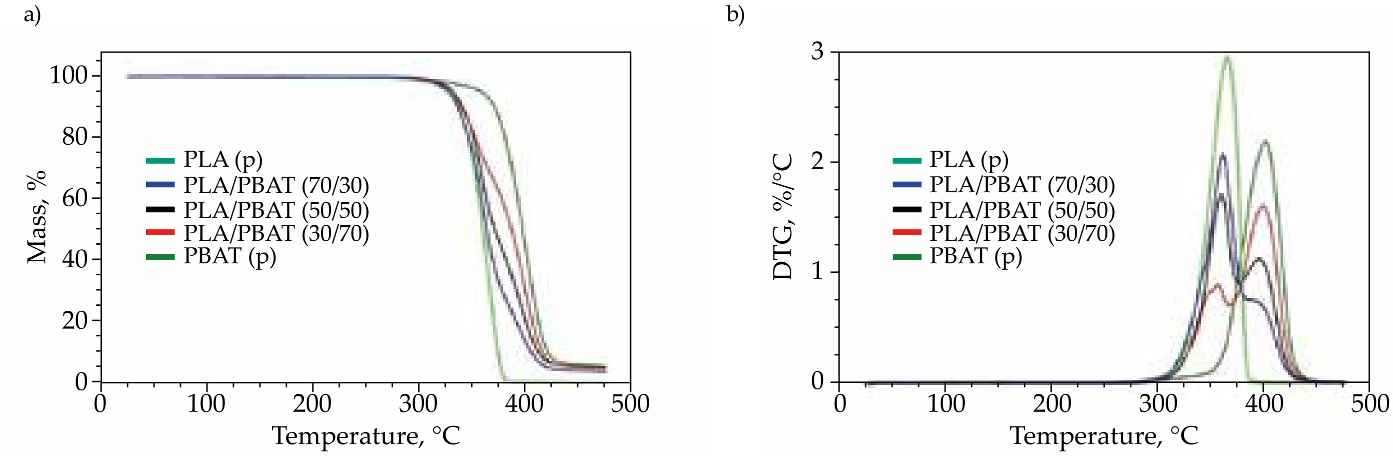

**Fig. 3. Thermogravimetric curves of PLA, PBAT and their blends: a) TG, b) DTG**

**Table 3. Blown film extrusion parameters for PLA/PBAT blends**

| PLA/PBAT wt%/wt% | Temperature °C | Screw speed rpm | Lay flat width mm | Thickness μm | BUR | DDR |
|---|---|---|---|---|---|---|
| PLA | 190–205 | 90 | 188 | 65 | 3.2 | 3.8 |
| 90/10 | 188–200 | 90 | 189 | 59 | 3.2 | 4.2 |
| 80/20 | 182–197 | 90 | 190 | 65 | 3.3 | 3.8 |
| 70/30 | 178–195 | 90 | 191 | 67 | 3.3 | 3.6 |
| 60/40 | 178–193 | 90 | 191 | 69 | 3.3 | 3.5 |
| 50/50 | 170–186 | 90 | 218 | 63 | 3.7 | 3.4 |
| 40/60 | 170–182 | 90 | 212 | 67 | 3.7 | 3.3 |
| 30/70 | 170–182 | 90 | 218 | 63 | 3.7 | 3.4 |
| 20/80 | 170–182 | 90 | 216 | 48 | 3.7 | 4.5 |
| 10/90 | 170–182 | 90 | 218 | 48 | 3.7 | 4.4 |
| PBAT(p) | 170–182 | 90 | 212 | 53 | 3.7 | 4.1 |
| PBAT | 170–182 | 90 | 214 | 66 | 3.7 | 3.3 |

**Fig. 4. Film blowing process of PLA/PBAT: a) 30/70, b) 50/50 c) 70/30**

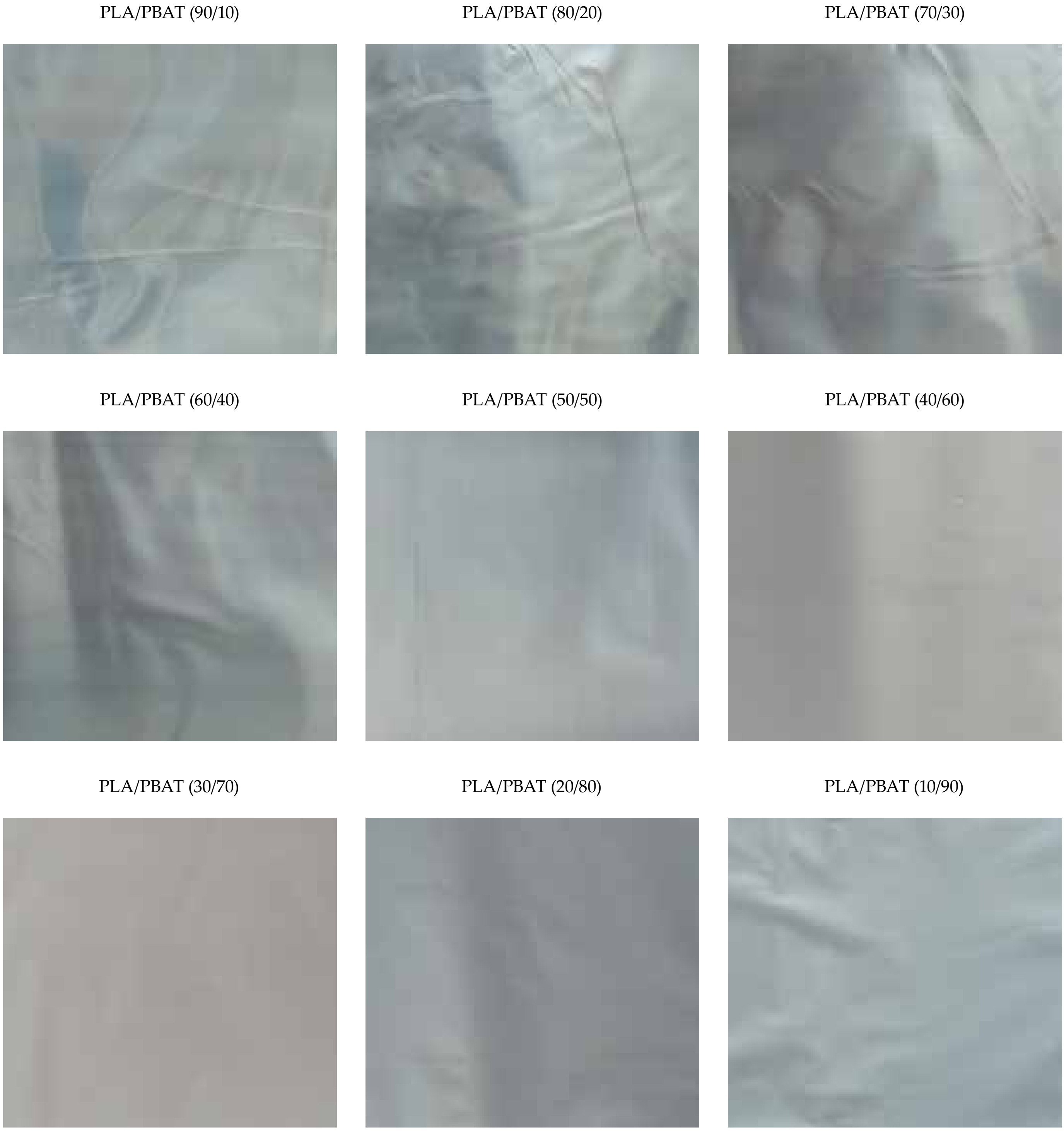

PLA/PBAT (90/10) PLA/PBAT (80/20) PLA/PBAT (70/30)

PLA/PBAT (60/40) PLA/PBAT (50/50) PLA/PBAT (40/60)

PLA/PBAT (30/70) PLA/PBAT (20/80) PLA/PBAT (10/90)

**Fig. 5. Surface of PLA/PBAT films**

strength of this polymer, but it could be carried out under appropriately selected processing conditions. In the case of PLA previously melted and regranulated (i.e., PLA(p)), the resulting film was wrinkled and showed large thickness variations, hence the blown film extrusion test was not performed. Instead, only the film obtained from pure PLA granulate was used as a reference sample during mechanical tests. The photos taken during the continuous and stable blowing process as well as the resulting PLA/PBAT films are shown in Figures 4 and 5, respectively.

## Morphology and miscibility of PLA/PBAT blends

The morphology of the blown PLA/PBAT films, including the size distribution of the polymer phases relative to each other, is shown in Fig. 6. As can be seen, PBAT is immiscible with PLA and phase separation occurs. However, the amount of PBAT fraction in PLA matrix affected the morphology. When PBAT content is in the range of 10–30 wt%, there are many discontinuities, holes, and fibrous structures in the PLA matrix, originating from PBAT domains.

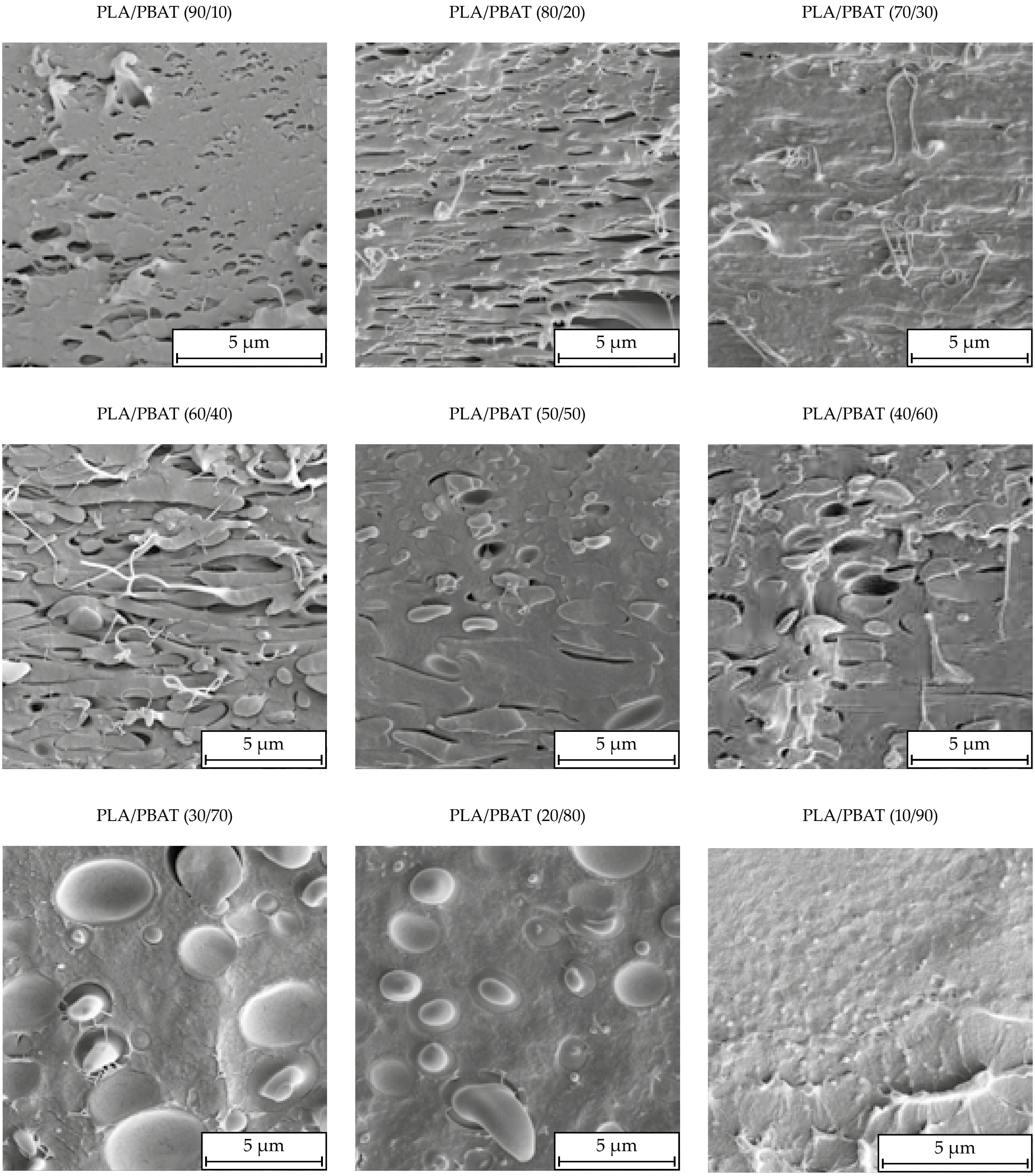
PLA/PBAT (90/10)
PLA/PBAT (80/20)
PLA/PBAT (70/30)
PLA/PBAT (60/40)
PLA/PBAT (50/50)
PLA/PBAT (40/60)
PLA/PBAT (30/70)
PLA/PBAT (20/80)
PLA/PBAT (10/90)

**Fig. 6. SEM images of PLA/PBAT films**

## Mechanical properties

The film with 10 wt% PBAT content was characterized by the same mechanical and processing properties as pure polylactide, but tensile strength and Young modulus of PLA/PBAT blends gradually decreased with increasing PBAT content (Fig. 7). It is worth noting that a significant increase in elongation occurred only when the PBAT content in the blends exceeded 30 wt% – below this threshold, the PBAT content was insufficient to obtain flexible films, which is not consistent with the results reported by Yeh *et al.* [16].

Elmendorf tear strength measurements were performed using a 200 g and 1600 g pendulum to obtain the

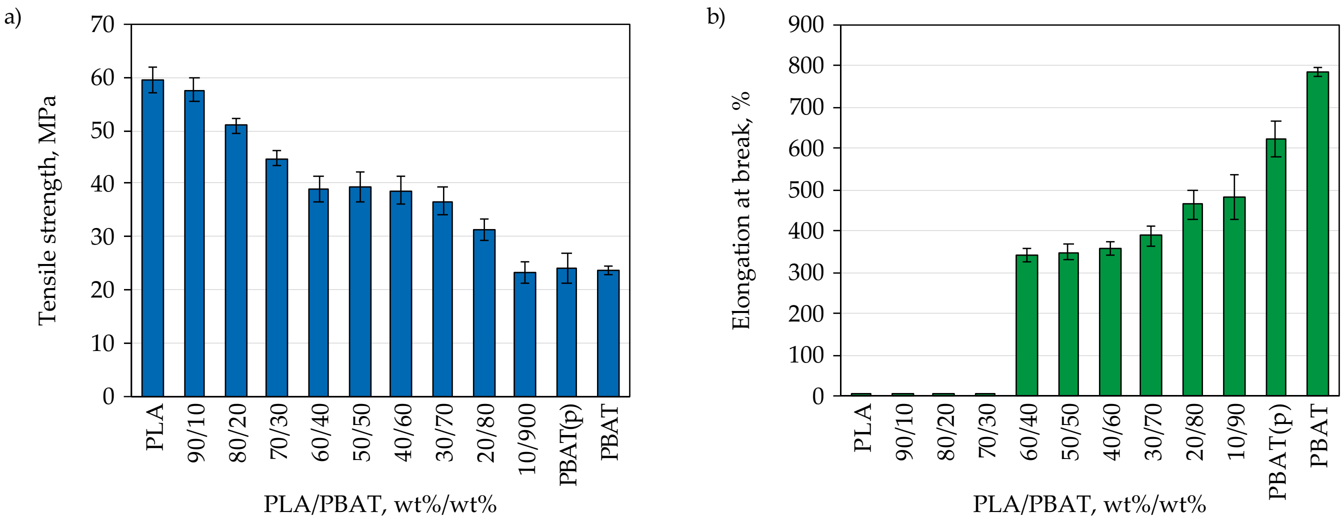

**Fig. 7. Mechanical properties of PLA/PBAT films: a) tensile strength, b) elongation at break**

**Table 4. Mechanical properties of PLA/PBAT films**

| PLA/PBAT wt%/wt% | Young modulus MPa | Tear resistance, N/mm | |
|---|---|---|---|
| | | 1600 g | 200 g |
| PLA | 2958 ± 99 | 2.5 ± 0.3 1) | 3.8 ± 0.2 1) |
| 90/10 | 2748 ± 84 | 5.1 ± 0.5 1) | 5.7 ± 0.6 1) |
| 80/20 | 2383 ± 58 | 11.5 ± 1.1 1) | 12.4 ± 0.7 |
| 70/30 | 2094 ± 68 | 18.5 ± 0.6 1) | 17.9 ± 0.6 |
| 60/40 | 1669 ± 47 | 14.7 ± 2.0 1) | 17.6 ± 2.0 |
| 50/50 | 1303 ± 38 | 10.7 ± 0.6 1) | 13.2 ± 1.8 |
| 40/60 | 993 ± 42 | 12.3 ± 2.8 1) | 11.1 ± 0.8 |
| 30/70 | 640 ± 21 | 42.7 ± 2.9 1) | 22.5 ± 0.7 |
| 20/80 | 264 ± 13 | 70.4 ± 2.6 | 28.1 ± 2.8 2) |
| 10/90 | 105 ± 7 | 73.1 ± 3.3 | 39.5 ± 1.9 2) |
| PBAT(p) | 75 ± 3 | 80.7 ± 3.2 | – 3) |
| PBAT | 73 ± 2 | 84.4 ± 2.6 | – 3) |

where: 1) the absorbed is <20% of the nominal energy of the pendulum, 2) the absorbed energy is >80% of the nominal energy of the pendulum, 3) the sample does not tear.

full measurement range. Some samples could not be measured according to PN-EN ISO 6383-2, i.e., the energy absorbed by them was outside the recommended limits (20–80% of the nominal pendulum energy). The results are summarized in Table 4. As can be seen, the tear propagation resistance of blown films increased with decreasing PLA content, and this phenomenon is particularly visible in the case of blends containing mainly PBAT.

## CONCLUSIONS

PLA/PBAT blends are immiscible in the entire range studied, as confirmed by FT-IR, DSC, and SEM analyses. It was shown that good quality films with a smooth surface can be obtained in blown film extrusion process when the PBAT content is at least 60 wt%. If the PBAT content was equal to or higher than 50 wt%, the blowing processing parameters were the same as for pure PBAT. Flexible films exhibiting optimal mechanical properties were obtained with PBAT content of 60 and 70 wt%. On the other hand, at lower PBAT contents (especially < 30 wt%), the films were wrinkled and inhomogeneous, and their elongation at break was like that of pure PLA. Such blends are not recommended for blown film extrusion.

## *ACKNOWLEDGEMENTS*

*This work was financially supported by The National Centre for Research and Development (LIDER X), grant number LIDER/36/0198/L-10/18/NCBR/2019 entitled: "The development of technology for obtaining the new biodegradable plastics based on thermoplastic starch for the films production".*

### *Authors contribution*

J.O. – conceptualization, methodology, writing - original draft, writing - review and editing, visualization, supervision, investigation, funding acquisition; W.S. – methodology, investigation; M.P. – investigation, visualization; M.D. – investigation, writing - review and editing; O.W. – investigation; K.S. – investigation; P.T. – investigation.

### *Funding*

This work was financially supported by The National Centre for Research and Development (LIDER X), grant number LIDER/36/0198/L-10/18/NCBR/2019 entitled: "The development of technology for obtaining the new biodegradable plastics based on thermoplastic starch for the films production".

### *Conflict of interest*

The authors declare no conflict of interest.

## REFERENCES

[1] Freeland B., McCarthy E., Balakrishnan R. *et al: Materials* **2022**, *15*, 2989. https://doi.org/10.3390/ma15092989
[2] Ranakoti L., Gangil B., Mishra S.K. *et al.: Materials* **2022**, *15*, 4312. https://doi.org/10.3390/ma15124312
[3] Auras R., Harte B., Selke S.: *Macromolecular Bioscience* **2004**, *4*, 835. https://doi.org/10.1002/mabi.200400043
[4] Farah S., Anderson D.G., Langer R.: *Advanced Drug Delivery Reviews* **2016**, *107*, 367. https://doi.org/10.1016/j.addr.2016.06.012
[5] *Pat. US* 8133558 (2012).
[6] Martin O., Averous L.: *Polymer* **2001**, *42*, 6209. https://doi.org/10.1016/S0032-3861(01)00086-6
[7] Wang L., Ma W., Gross R.A. *et al.: Polymer Degradation and Stability* **1998**, *59*, 161. https://doi.org/10.1016/S0141-3910(97)00196-1
[8] Nam K., Kim S.G., Kim D.Y. *et al.: Polymers* **2024**, *16*, 518. https://doi.org/10.3390/polym16040518
[9] Jiang Y., Yan C., Wang K. *et al.*: *Materials* **2019**, *12*, 1663. https://doi.org/10.3390/ma12101663
[10] Nofar M., Sacligil D., Carreau P.J. *et al.: International Journal of Biological Macromolecules* **2019**, *125*, 307. https://doi.org/10.1016/j.ijbiomac.2018.12.002
[11] Jian J., Xiangbin Z., Xianbo H.: *Advanced Industrial and Engineering Polymer Research* **2020**, *3*, 19. https://doi.org/10.1016/j.aiepr.2020.01.001
[12] Hongdilokkul P., Keeratipinit K., Chawthai S. *et al.: IOP Conference Series: Materials Science and Engineering* **2015**, *87*, 012112. http://dx.doi.org/10.1088/1757-899X/87/1/012112
[13] Carbonell-Verdu A., Ferri J.M., Dominici F. *et al.: eXPRESS Polymer Letters* **2018**, *12*, 808. https://doi.org/10.3144/expresspolymlett.2018.69
[14] Jiang L., Wolcott M.P., Zhang J.: *Biomacromolecules* **2006**, *7*, 199. https://doi.org/10.1021/bm050581q
[15] Su S., Duhme M., Kopitzky R.: *Materials* **2020**, *13*, **4897.** https://doi.org/10.3390/ma13214897
[16] Yeh J.-T., Tsou C.-H., Huang C.-Y. *et al.: Journal of Applied Polymer Science* **2010**, *116*, 680. https://doi.org/10.1002/app.30907
[17] Su S.: *Materials Research Express* **2022**, *9*, 025308. https://dx.doi.org/10.1088/2053-1591/ac55c7
[18] Arruda L.C., Magaton M., Bretas R.E.S. *et al.: Polymer Testing* **2015**, *43*, **27.** https://dx.doi.org/10.1016/j.polymertesting.2015.02.005
[19] Pietrosanto A., Scarfato P., Maio L.D. *et al.: Materials* **2020**, *13*, 5395. https://doi.org/10.3390/ma13235395
[20] Pietrosanto A., Apicella A., Scarfato P. *et al.: Polymers* **2022**, *14*, 2759. https://doi.org/10.3390/polym14142759
[21] Tsuji H., Ikada Y.: *Polymer* **1995**, *36*, 2709. https://doi.org/10.1016/0032-3861(95)93647-5
[22] Azevedo J.V.C., Ramakers-von Dorp E., Grimmig R. *et al.: Polymers* **2022**, *14*, 1939. https://doi.org/10.3390/polym14101939
[23] Xiao H., Lu W., Yeh J.-T.: *Journal of Applied Polymer Science* **2009**, *112*, 3754. https://doi.org/10.1002/app.29800

*Received 25 V 2024.*
*Accepted 26 VI 2024.*

---

## Rapid Communications

Przypominamy Autorom, że publikujemy artykuły typu **Rapid Communications – prace oryginalne wyłącznie w języku angielskim** (o objętości 4–5 stron maszynopisu z podwójną interlinią, zawierające 2–3 rysunki lub 1–2 tabele), którym umożliwiamy szybką ścieżkę druku (do 3 miesięcy od chwili ich otrzymania przez Redakcję). Artykuł należy przygotować wg wymagań redakcyjnych zamieszczonych we wskazówkach dla P.T. Autorów.

* * *

We remind Authors that we publish articles of the **Rapid Communications** type **– the original papers, in English only** (with a volume of 4-5 pages of double-spaced typescript, containing 2–3 figures or 1–2 tables), which allow a fast print path (up to 3 months from when they are received by the Editorial Board). The article should be prepared according to the editorial requirements included in the Guide for Authors.